

Going Nonlinear

FOCUSED
ISSUE FEATURE

*Charles Baylis, Robert J. Marks II,
Josh Martin, Hunter Miller, and Matthew Moldovan*



Since the advent of the nonlinear vector network analyzer (NVNA), microwave engineers have become familiar with new terminology regarding nonlinear network parameters such as “X-parameters” (registered trademark of Agilent Technologies) [1], “S-functions,” [2]–[4], and “waveform engineering/the Cardiff model” [5], as well as new types of equipment used to perform nonlinear characterizations [6]. These nonlinear network parameter approaches have been developed by Root and Verspecht [1], Verbeyst and Vanden Bossche [2]–[4], and Tasker [5]. Equipment is now commercially available to measure these parameters. To date, X-parameters and S-functions have been predominately used to describe amplifiers in system level simulations. Waveform engineering with the Cardiff model has focused on transistor-level amplifier design. Understanding these behavioral modeling approaches allows their application as an effective and time-saving tool for nonlinear power amplifier design. This article examines the X-parameters and S-functions in an effort to provide a working knowledge that will also apply to understanding the other aforementioned approaches. (An example of X-parameters applied to transistor modeling is given in “X-parameters Work for Transistors Too!” by Betts et. al.) While this model description takes a lesser-known amplifier design perspective, it applies equally to modeling

Charles Baylis (Charles-Baylis@baylor.edu), Robert J. Marks II, Josh Martin, Hunter Miller, and Matthew Moldovan are with Wireless and Microwave Circuits and Systems Program, Department of Electrical and Computer Engineering, Baylor University, Texas.

Digital Object Identifier 10.1109/MMM.2010.940102

Date of publication: 9 March 2011

amplifiers at the system-design level, which has been extensively proven.

The Amplifier Design Problem

The basic amplifier design problem is illustrated in Figure 1 [7]. An active device (transistor-based or vacuum-tube-based along with its bias network) is specified, and the input and output matching networks are chosen to meet a set of design criteria, possibly including gain, noise, output power, efficiency, and linearity. For signals that are sufficiently small such that the transistor is operated linearly, the small-signal design can be based solely upon small-signal S-parameters. (Noise parameters of the device are also necessary for plotting of noise figure circles on the Smith Chart. Noise parameters are not considered in this article.) The approach is simple and equation-based, and an initial design can be reached relatively quickly by performing a small number of measurements. The final design consists of values for the source and load reflection coefficients (Γ_s and Γ_L), which are then implemented through appropriate matching network design.

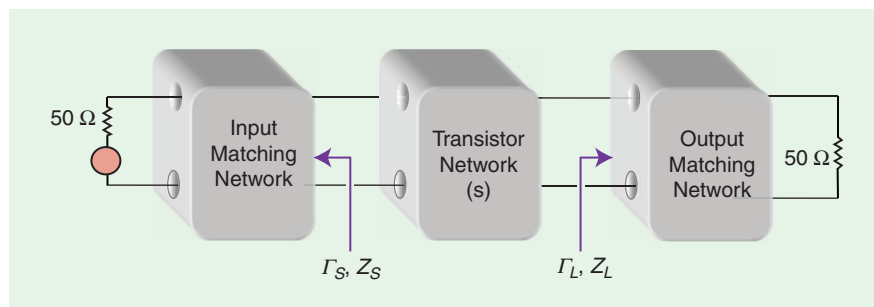


Figure 1. Conceptual block diagram of the microwave amplifier design problem [8]. The input and output matching networks are designed to present reflection coefficients, allowing optimization of gain, power, efficiency, noise, and stability.

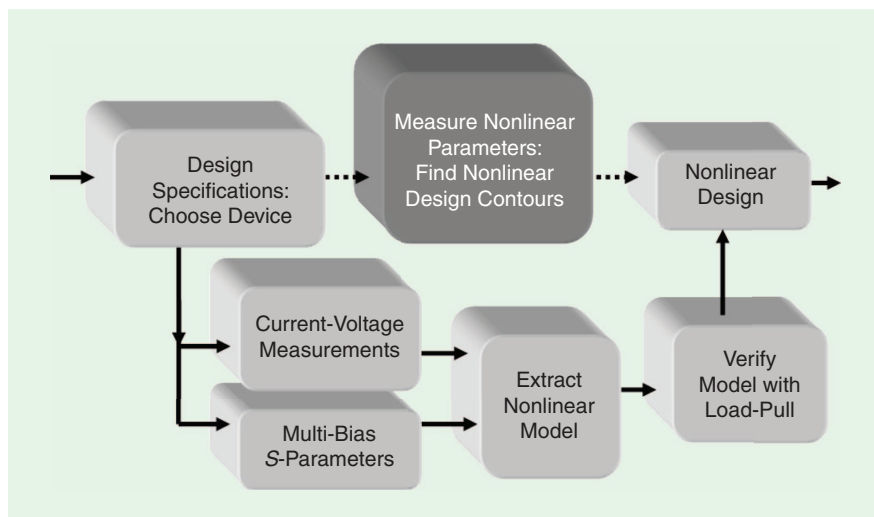


Figure 2. Nonlinear design flowchart. The use of nonlinear network parameters creates a measurement-based model for the device that, in many cases, can save time and effort normally required to perform a full nonlinear model extraction.

For large-signal power amplifiers, the same block diagram is used; however, the transistor no longer can be accurately characterized by its S-parameters alone. The signal is large enough to traverse a significant range of operation with respect to the limitations of the device. The nonlinearities in the system cause frequency conversions, meaning that a large-signal input will generate outputs that vary periodically with the same fundamental frequency but contain harmonic content at frequencies other than the fundamental. The S-parameters do not have the structure to describe the harmonic transfer of the nonlinear transistor; however, if the S-parameters can be extended to describe the harmonic transfer of the system under a nonlinear operating condition, it may be possible to simplify the design procedure for some specific cases. Without the availability of nonlinear network parameters, a complex nonlinear modeling approach or empirical source/load-pull approach must be used to describe the device behavior, which then feeds into the design of the input and output matching networks. Nonlinear device models for present-day active devices contain multiple parameters and require current-voltage, multiple-bias S-parameter, and load-pull measurements to extract and verify the model.

Figure 2 shows a block diagram of the nonlinear amplifier design cycle. The goal of using nonlinear network parameters is to develop a simple, parameter-based design approach that will circumvent the need for traditional compact (or physical in some cases) nonlinear model extraction in some cases and provide the necessary information to directly find the values of Γ_s and Γ_L to meet the design requirements for gain, output power, efficiency, and linearity.

Small-Signal S-Parameters

The formulation of the large-signal X-parameters degenerates to the small-signal S-parameters under small-signal conditions. In S-parameter characterization, incident and reflected voltage wave amplitudes are measured at each of the ports. Figure 3 shows a block diagram with the *a* waves going into the network and the *b* waves leaving the network.

X-Parameters Work for Transistors Too!

by Loren Betts, Dylan T. Bepalko, and Slim Boumaiza

While much of the early focus of measurement-based behavioral models was aimed at system-level models for integrated assemblies, such as amplifiers, mixers, etc., X-parameters, S-functions, and the Cardiff model have proven to be as powerful a design tool with transistor-level models in circuit design [S1]–[S3]. Here we demonstrate X-parameter measurements and simulations on an unmatched, GaN high electron mobility transistor (HEMT), power transistor. X-parameters were measured at 1.2 GHz with three harmonics, an input power range of 10–32 dBm, a 400 μ s pulse width, and a 1% duty cycle. Because of the high power levels associated with this device and measurement, an external test setup was used that protected the instrument and provided the necessary dynamic range and frequency coverage. The device bias point is $V_{ds} = 28$ V and $V_{gs} = -2.87$ V, which

sets $I_{dsq} = 400$ mA. Because the power device is not matched to 50Ω , both input and output tuners were used. The input tuner's function is to deliver more effectively an input RF voltage to the device at the fundamental frequency, so it is not necessary to measure with multiple source states. The input voltage variation is achieved by sweeping the input power, and source impedance variation in a circuit design is handled with the model formulism. However, it is necessary to measure over multiple load tuner states (the X-parameter model was indexed over 90Γ in the top left quadrant of the Smith Chart at a $.07 \Gamma$ separation). Since the X-parameter extraction procedure performs swept-phase measurements at the harmonic frequencies, any variations of the harmonic source and load impedances are implicitly defined inside the X-parameter model. Therefore,

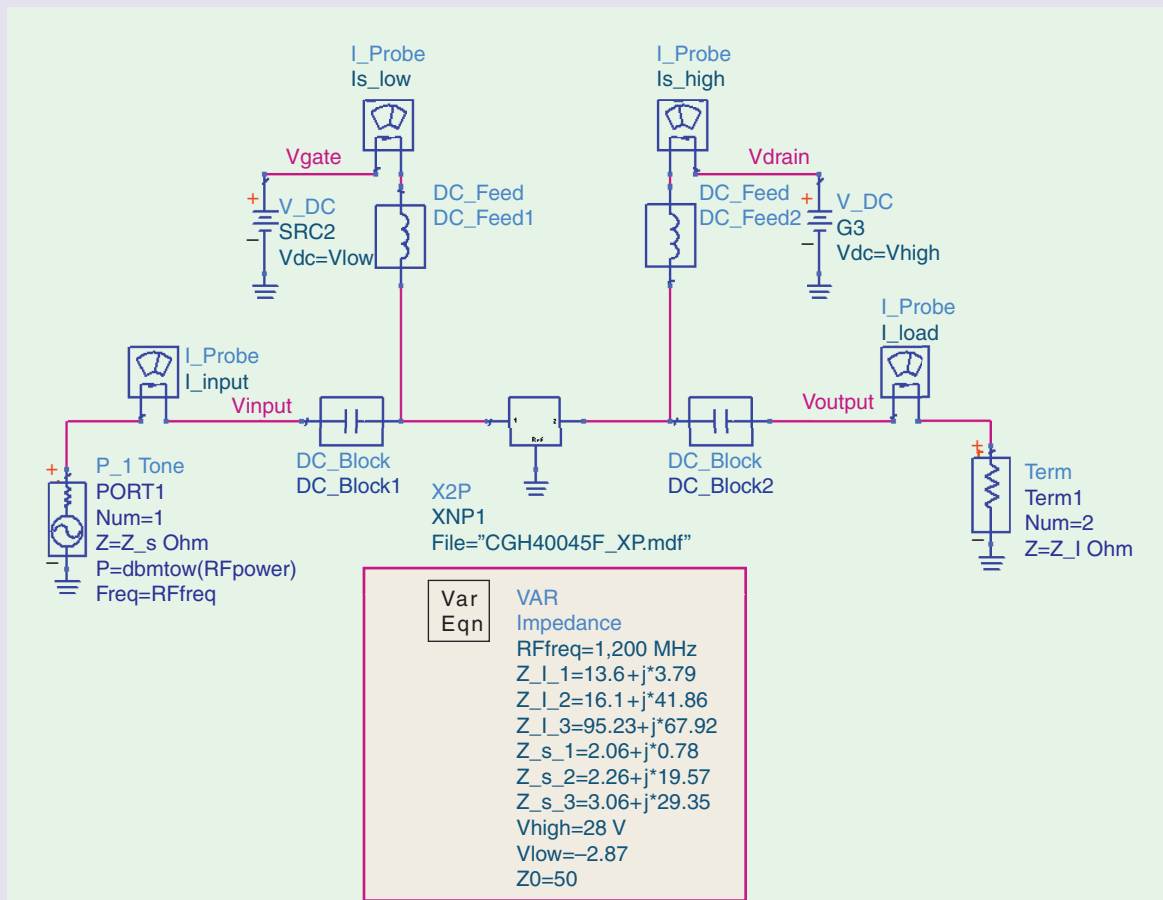


Figure S1. High power GaN HEMT simulation using an X-parameter model with bias values and source and load impedances set to match the measurement conditions.

Loren Betts (loren_betts@agilent.com) is with Agilent Technologies, Santa Rosa, California. Dylan T. Bepalko and Slim Boumaiza are with Agilent Technologies and the University of Waterloo, Ontario, Canada.

independent control of the harmonic impedances using tuners is not necessary for the X-parameter model extraction.

To demonstrate the functionality of a device-level X-parameter model over the expected stimulus/response range, the simulated performance of the device using the X-parameter model is compared to the measured performance of the actual component. The comparison was carried out in an impedance environment that was different from that in which the model was extracted; however, for the comparison it is critical the measured and simulated impedance terminations are identical. (If the simulation impedances are not matched at the fundamental, the basic load-line is not valid, and the power, gain, etc. will be incorrect. With mismatches at the harmonics, the class of operation can be very different, which can produce large errors in the simulated current and efficiency.) At the fundamental frequency, the application of a physical impedance from a tuner was used to generate load-dependent X-parameters. The fundamental frequency impedances chosen for the measurements were not the same physical impedances as that used to create the X-parameter model but were contained inside a rectangular impedance grid defined during the X-parameter measurements. As was mentioned previously, the component behavior versus harmonic source and load impedances is implicitly defined in the X-parameter model and identified during the X-parameter measurement. Therefore, the X-parameter model is valid over a full range of reflection coefficients at the harmonic source and load impedances defined by the X-parameter measurement. The impedances are shown in the simulation network in Figure S1. Figure S2 illustrates a comparison between the measured and simulated power delivered to the load and the device current. This example shows the ability of the model to simulate device-level performance. This model

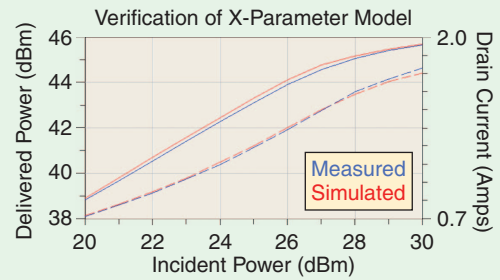


Figure S2. Simulated and measured power delivered to the load (solid lines) and device current (dashed lines) as a function of input power for a GaN HEMT. The simulation employs an X-parameter, measurement-based behavioral model.

would be a very useful tool in the design of a high-power circuit employing this device, both for the single-tone case demonstrated here as well as a modulated or multi-tone signal. For the multi-tone and modulated cases, one must make the narrow-band approximation, where one assumes the single-tone performance is constant over the bandwidth of the signal when using an X-parameter model measured with a single-tone drive signal on the input. The utility of a measurement based model is especially true in cases like this where the device is a commercially available transistor, where a compact model is not available or is complicated by package effects.

References

- [S1] J. Horn, D. E. Root, and G. Simpson, "GaN device modeling with X-parameters," in *2010 IEEE CSIC Symposium Dig.*, Monterey, CA, Oct. 2010, pp. 39–42.
- [S2] M. Myslinski, F. Verbeyst, M. Vanden Bossche, and D. Schreurs, "S-Functions extracted from narrow-band modulated large-signal network analyzer measurements," in *74th ARFTG Conf. Dig.*, Broomfield, CO, Dec. 2009, pp. 107–114.
- [S3] P. J. Tasker, "Practical waveform engineering," *IEEE Microwave Mag.*, vol. 10, no. 7, pp. 65–76, Dec. 2009.

The S-parameter equations define the waves leaving each port in terms of all waves entering the network. For two ports,

$$\begin{aligned} b_1 &= S_{11}a_1 + S_{12}a_2 \\ b_2 &= S_{21}a_1 + S_{22}a_2. \end{aligned} \quad (1)$$

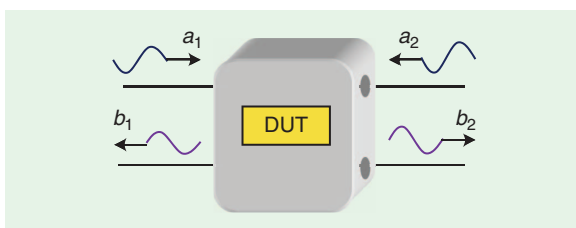


Figure 3. S-parameter characterization diagram.

To measure the S-parameters, measurements are taken at each port while ensuring that no wave is entering the nonexcited port, meaning that the nonexcited port is terminated in the characteristic impedance Z_0 (usually 50 Ω).

$$S_{11} = \left. \frac{b_1}{a_1} \right|_{a_2=0} \quad S_{21} = \left. \frac{b_2}{a_1} \right|_{a_2=0} \quad S_{12} = \left. \frac{b_1}{a_2} \right|_{a_1=0} \quad S_{22} = \left. \frac{b_2}{a_2} \right|_{a_1=0}. \quad (2)$$

These measurements are performed with a vector network analyzer (VNA) by exciting the ports of the device under test (DUT) one at a time and measuring

the magnitude and phase of the output wave at the appropriate port.

For a device with G ports, the general expression for the output voltage wave from port e in terms of the S-parameters is given by

$$b_e = \sum_{g=1}^G S_{eg} a_g. \quad (3)$$

Fundamentals of X-Parameters and S-Functions

The X-parameters represent a linear approximation in the Fourier series coefficient domain of a nonlinear function as it varies small distances around a large-signal operating condition [9]. These have been derived based on the polyharmonic distortion (PHD) model introduced by Verspecht et al. [10]. The X-parameters can be applied to a time-invariant system in which output signals vary periodically with the same fundamental period as the input signal. The description of an output wave B_{ef} at port e and harmonic f is given as a function of a large-signal input at harmonic 1 (the fundamental) and port 1 (A_{11}) and small perturbation signals at all ports g and harmonics h by the defining equation for the X-parameters [1]

$$B_{ef} = X_{ef}^{(F)}(|A_{11}|)P^f + \sum_{g,h \neq 1,1} X_{ef,gh}^{(S)}(|A_{11}|)P^{f-h}a_{gh} + \sum_{g,h \neq 1,1} X_{ef,gh}^{(T)}(|A_{11}|)P^{f+h}a_{gh}^*, \quad (4)$$

where

$$P = e^{j\angle(A_{11})}.$$

The X-parameters in (4) can be viewed as a generalization of the S-parameters in (3).

Another commonly used approach to linearly approximating the Fourier series coefficient changes of nonlinear system outputs is the S-function approach presented by Myslinski et al. in [3]:

$$b'_{ph} = S_{f_{ph11}}|a_{11}| + \sum_{i,j \neq 1,1} (S_{f_{phij}}a'_{ij} + S_{f_{c_{phij}}}(a'_{ij})^3),$$

with

$$x'_{ph} = x_{ph} e^{-jh\angle(a_{11})} = x_{ph} P^{-h}, \quad (5)$$

where b'_{ph} is the phase-normalized output voltage wave at port p and harmonic h , and i and j are the input port and input harmonic, respectively. The S-function construction is very similar to that of the S-parameters, with three terms: the first describing a response to a large-signal input and the second and third terms inside the summation describing the change in response due to perturbations at the ports and harmonics. As the construction of the two approaches is similar, the X-parameter approach of (4)

will be discussed thoroughly in this article, with the understanding that similar analysis approaches can be used to find the S-functions. Specifically, from (4) and (5), the relationships between the X-parameter and S-function equation terms are

$$\begin{aligned} S_{f_{e11}}|a_{11}| &= X_{ef}^{(F)}, \\ S_{f_{efgh}} &= X_{ef,gh}^{(S)} \quad \text{for } i \neq 1, j \neq 1, \\ S_{f_{efgh}} &= X_{ef,gh}^{(S)} \quad \text{for } i \neq 1, j \neq 1. \end{aligned} \quad (6)$$

The terms are exceedingly similar, and both the S-functions and X-parameters are functions of the large-signal input; meaning that the matrices change (in general) for a change in large-signal input amplitude.

What do the terms in the X-parameter equation mean? The first term in (4) represents the large-signal operating condition output due to an input signal consisting of a large-signal, zero-phase cosine wave A_{11} at port 1 and harmonic 1 (the fundamental). The first term in the equation contains a vector that allows conversion from the large-signal input to the magnitude and phase at the output of each harmonic. As in the case of S-parameters, these terms represent phasors; therefore it is important to consider that to change frequencies, the output phase must be multiplied by the ratio of the frequency of the output harmonic under consideration to that of the fundamental. This is the reason for the P^f type term in (1). Borrowing from the fast Fourier transform (FFT) algorithm, P is dubbed the "twiddle factor" [11]. It allows parameters to be adjusted to a phase shift in the stimulus. Thus the $X_{ef}^{(F)}$ matrix simply gives the output voltage waveform phasor values at all combinations of output port and harmonic. Because the system is nonlinear, each set of X-parameters is a function of the magnitude of the sinusoidal input, $|A_{11}|$. If this amplitude changes, the X-parameters change.

The second and third terms in (4) describe the change in the traveling voltage wave leaving port e at harmonic f due to small-signal perturbation signals that are input to each port and stimulate each harmonic while the large-signal input A_{11} continues to be applied. Because the application of the large-signal input A_{11} drives the system into nonlinear operation and results in an output containing harmonics, the addition of a small-signal periodic input will result in mixing of the small-signal with the fundamental and harmonic frequencies produced by the large-signal input. This will excite the frequency conversion in the system that we wish to characterize. Thus, the ability of the system to generate harmonics is represented by $X^{(F)}$, while the ability of the system to perform frequency conversion of small perturbation signals is represented by $X^{(S)}$ and $X^{(T)}$. The fact that two matrices are needed is a result of the possibility

shown by Verspecht that the nonlinearity is nonanalytic [10], meaning that B_{ef} cannot be expressed as a function of the input signal a_{gh} alone, but is also a separate function of its conjugate, a_{gh}^* [9, 12]. Because real signals are produced in the laboratory, the Fourier series coefficients are conjugately symmetric [13]. Thus, if a_{gh} is the phasor associated with the positive frequency component of the exponential Fourier series then, because the signal is real, a_{gh}^* is the coefficient associated with the corresponding negative frequency. The matrix $X^{(S)}$ represents the conversion from harmonics h to harmonics f at the output, and the matrix $X^{(T)}$ represents the conversion from harmonics $-h$ in the exponential Fourier spectrum to the same harmonic f (the $X^{(S)}$ matrix represents coupling between positive or negative harmonics, while the $X^{(T)}$ matrix represents “cross-coupling” from negative to positive harmonics and vice versa). The term converting from harmonic h will convert $f-h$ harmonics in frequency, and the term converting from harmonic $-h$ will convert $f+h$ harmonics in frequency.

“Interpretation of X-parameters as Incremental Small-Signal Harmonic Coupling” discusses in more mathematical detail how the X-parameters can be interpreted as incremental small-signal harmonic coupling.

Measuring the Nonlinear Network Parameters

A method to measure X-parameters or S-functions with a small number of experiments is the “off-frequency” approach [10]. This technique places the perturbation frequencies at a slight offset from the desired input frequency. With all noninput ports terminated in Z_0 , a small perturbation signal is input at harmonic g and port h . Because (by necessity of real laboratory measurements) the signal must be real, a_{gh} and a_{gh}^* are produced simultaneously. The input frequency of the small perturbation is slightly offset from the harmonic of the input at frequency $g\omega_0 + \Delta\omega$. The

frequency offset allow the terms resulting from a_{12} to be distinguished from a_{12}^* . The results of this perturbation input are then measured at port e and harmonic f . As an example, consider the test configuration to find the X-parameter pair $X_{23,12}^{(S)}$ and $X_{23,12}^{(T)}$. This pair gives information about the transmission from port 1, harmonic 2 to port 2, harmonic 3. The input wave a_{12} for this configuration is a tone slightly above the second harmonic at port 1, shown in Figure 4. The dashed frequency content in Figure 4 shows the harmonics already present due to the large-signal input signal $|A_{11}|$ (these plots are similar to the explanations provided in [1]). Because generating a real signal consists of generating frequency content at both the positive and corresponding negative frequency values of the sinusoidal frequency, positive and negative frequency terms will appear in the exponential Fourier spectrum that are complex conjugates of each other.

Because the system is already pressed into nonlinear operation by the large-signal input A_{11} , the small-signal perturbation signal composed of a_{12} and a_{12}^* will mix with the harmonics already present in the signal. To find the two X-parameters desired, it is necessary to measure the output frequency content due to this perturbation at port 2 and harmonic 3: b_{23} . How will content be generated at this frequency and port? The content will be generated due to the mixing of a_{12} and a_{12}^* with the harmonics. During the mixing process, the exponential terms containing the frequencies will multiply, causing resulting exponential expressions with frequencies equal to the sums of the initial frequencies. A term will be generated at $3\omega_0 + \Delta\omega$ through an addition of the a_{gh} perturbation frequency $2\omega_0 + \Delta\omega$ to the fundamental term at ω_0 . In addition, a term will be generated at $3\omega_0 - \Delta\omega$ by the addition of the a_{gh}^* perturbation frequency to the fifth-harmonic frequency $5\omega_0$. The output spectrum is shown in Figure 5.

Introducing these components into a nonlinear system will result in outputs at appropriate sum frequencies that will lie directly adjacent to the output harmonic. The input cosine, in this case at frequency $2\omega_0 + \Delta\omega$ is split into two complex exponential components: one at $2\omega_0 + \Delta\omega$ (this is a_{12}) and one at $-2\omega_0 - \Delta\omega$ (this is a_{12}^*). Adding these frequencies to appropriate harmonics already existing in the system will generate terms above (from a_{12}) and below (from a_{12}^*) the harmonic frequency. Based on the magnitude and phase of these terms, the X-parameter governing this frequency conversion can

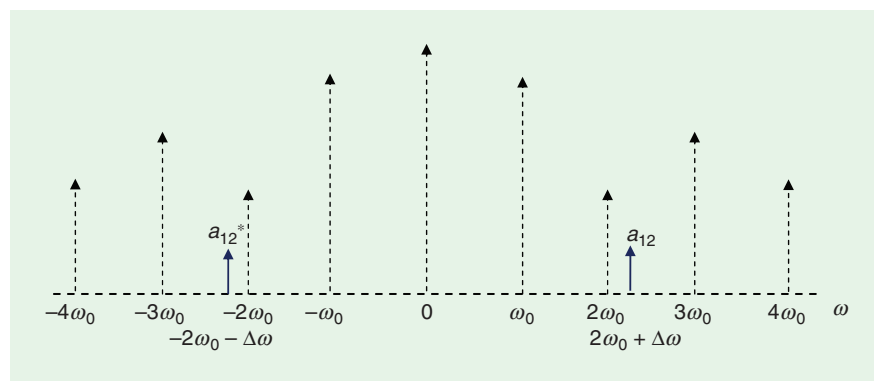


Figure 4. Frequency content of the perturbation signal a_{12} (solid lines) with the results of the large-signal input (dashed lines) shown. The perturbation tones a_{12} and a_{12}^* comprise a cosine perturbation at the second harmonic and can be slightly offset from the harmonic to allow the terms resulting from a_{12} to be easily distinguished from a_{12}^* .

Interpretation of X-Parameters as Incremental Small-Signal Harmonic Coupling

X-parameters can be nicely interpreted as a linearization of the cross coupling of harmonics, as presented in [9]. The linearized incremental contributions from each input port are superimposed to generate the composite response.

Let's assume we have G ports and a single cosine stimulus at port one. The stimulus provides an operating point around which the X-parameters are calculated. If the amplitude or frequency of the stimulus is changed, the operating point is changed and new X-parameters must be recalculated (or remeasured). The X-parameters capture the effects of incremental changes in harmonics on the system operation. The harmonic coupling resulting from the nonlinearity can therefore be treated as a small signal phenomenon.

Denote the operating point of the response at port e by the large signal $\beta_e(t)$ and let harmonic f of this signal be denoted by β_{ef} . Consider, then, Figure S3 where a small-signal stimulus at port g denoted by $a_g(t)$ gives a response $b_{eg}(t)$ at port e . The g subscript is necessary on $b_{eg}(t)$ because there will be contributions from other ports in the total determination of the response at port e . Denote the h th harmonic of $a_g(t)$ by a_{gh} . What is the contribution of a_{gh} alone to the f th harmonic of $b_{eg}(t)$? Denote this contribution by $b_{ef,gh}$. Under a small-signal linear model, $b_{ef,gh}$ will be proportional to a_{gh} . The proportionality constant is the slope of the nonlinearity at the operating point. Hence, the contribution from a_{gh} is $b_{ef,gh} = (\partial b_{ef,gh} / \partial a_{gh}) a_{gh}$, where the partial derivative is taken at the network's operating point. Under the small-signal linearity assumption, summing the contributions of all of the harmonics at port g gives the total harmonic signal at port e due to the port g stimulus, which we will denote by

$$b_{ef,g} = \sum_{h=-\infty}^{\infty} b_{ef,gh} = \sum_{h=-\infty}^{\infty} \frac{\partial b_{ef,gh}}{\partial a_{gh}} a_{gh}.$$

Summing over the contributions from all G ports gives the perturbation

$$b_{ef} = \sum_{g=1}^G \sum_{h=-\infty}^{\infty} \frac{\partial b_{ef,gh}}{\partial a_{gh}} a_{gh}. \quad (S1)$$

In this form, the relationship is analytic. Since, however, all signals are assumed real, the Fourier series coefficients are conjugately symmetric [13], and we can write

$$a_{g,h}^* = a_{g,-h}.$$

Thus (S1) can be written in nonanalytic [10], conjugate form as

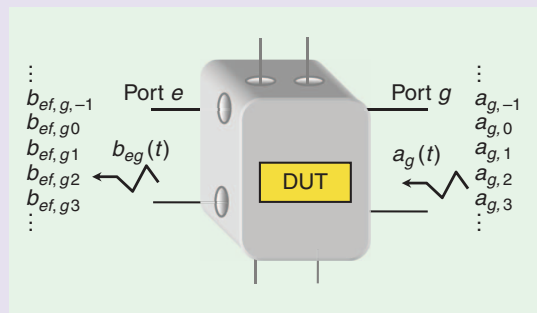


Figure S3. Illustration of X-parameters as a small-signal model of cross-harmonic coupling. Only the incremental contribution of the stimulus $a_g(t)$ in port g to the output $b_e(t)$ at port e is considered for each measurement. Each stimulus harmonic generally contributes to each response harmonic. The matrix of these small-signal contributions is the foundation for the X-parameters.

$$b_{ef} = \sum_{g=1}^G \left[\frac{\partial b_{ef,go}}{\partial a_{go}} a_{go} + \sum_{h=1}^{\infty} \frac{\partial b_{ef,gh}}{\partial a_{gh}} a_{gh} + \sum_{h=1}^{\infty} \frac{\partial b_{ef,g,-h}}{\partial a_{g,h}^*} a_{g,h}^* \right]. \quad (S2)$$

To this small-signal model of cross-harmonic coupling, we add the large-signal operating point to get the composite signal $\tilde{B}_{ef} = \beta_{ef} + b_{ef}$. X-parameters do not consider DC terms, so $(\partial b_{ef,go} / \partial a_{go}) a_{go}$ in (S2) is dropped. The result, then, is,

$$\tilde{B}_{ef} = \beta_{ef} + \sum_{g=1}^G \left[\sum_{h=1}^{\infty} \frac{\partial b_{ef,gh}}{\partial a_{gh}} a_{gh} + \sum_{h=1}^{\infty} \frac{\partial b_{ef,g,-h}}{\partial a_{g,h}^*} a_{g,h}^* \right]. \quad (S3)$$

This is the description of the circuit when the fundamental stimulus is a zero-phase cosine. Note that, if $k(t)$ with period T has harmonic amplitudes k_n , then $k(t - \tau)$ has harmonic amplitudes of $k_n e^{-j2\pi n \tau / T} = k_n P^n$, where $P = e^{-j2\pi \tau / T}$ is the "twiddle factor" in (5). A phase delay in the excitation therefore renders $\partial b_{ef,gh} / \partial a_{gh}$ to $(\partial b_{ef,gh} / \partial a_{gh}) P^{f-h}$ and $\partial b_{ef,g,-h} / \partial a_{g,h}^*$ to $(\partial b_{ef,g,-h} / \partial a_{g,h}^*) P^{f+h}$. With these phase terms, (S3) becomes

$$B_{ef} = \beta_{ef} P^f + \sum_{g=1}^G \left[\sum_{h=1}^{\infty} \frac{\partial b_{ef,gh}}{\partial a_{gh}} P^{f-h} a_{gh} + \sum_{h=1}^{\infty} \frac{\partial b_{ef,g,-h}}{\partial a_{g,h}^*} P^{f+h} a_{g,h}^* \right]. \quad (S4)$$

This is equivalent to the X-parameter equation in (4). The X-parameter description is a linearization, in that it superimposes all harmonic frequency conversions around a large-signal operating point. The accuracy of this approach (or lack thereof) is related to the severity of the nonlinearity of the system and the accuracy of the small-signal approximation for the perturbation signals.

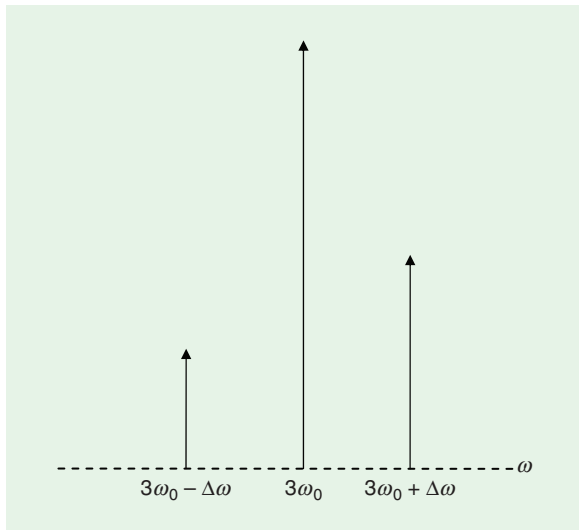


Figure 5. Frequency content of the output component B_{23} . The frequency component above the harmonic results from a_{12} and the component below comes from a_{12}^* . The signals at $3\omega_0 - \Delta\omega$ and $3\omega_0 + \Delta\omega$ are used to model the frequency conversion of the nonlinear system in its operating state.

be calculated. Because of the use of phasors in a frequency conversion system, however, part of the phase change will be due to the change in frequency (and hence the relationship of phase to time delay). This must be taken into account by adding a phase equal to an integer multiple of the phase of A_{11} to the phase of the term; the integer multiple should be equal to the number of harmonic frequencies of the translation that occurs in the exponential Fourier spectrum. For example, (4) defines the phase of the large-signal input; this phase must be multiplied by the number of harmonics in the frequency conversion, causing P to be raised to an integer exponential equal to the number of harmonics that the input frequency is upconverted.

Note that the phase translated for the term associated with a_{gh} is less than the phase translated for $a_{gh}^* f - h$ for the example considered here ($f = 3, h = 2$) is 1; this is consistent with the fact that the parameter $X_{23,12}^{(S)}$ governs a change in frequencies from the second to the third harmonic. $f + h$ is $3+2 = 5$ for this problem. This is the number of harmonic frequencies involved in the translation involving a_{gh}^* ; note that this translation occurs from a negative value of ω to a positive value of ω Ref. [9] provides further information about the Jacobian mathematics involved in this translation.

Because of the fact that the small-tone frequencies are slightly offset from the harmonics produced by the large-signal input, only one vector measurement is required for obtaining both $X_{23,12}^{(S)}$ and $X_{23,12}^{(T)}$. This is because the value of $X_{23,12}^{(S)}$ can be obtained by examining the frequency slightly higher than the harmonic and the value of $X_{23,12}^{(T)}$ can be obtained by examining the frequency slightly lower than the harmonic.

Many commercially available solutions for X-parameter measurement today actually employ the “on-frequency” technique. In this approach, the small-signal perturbations are placed at frequencies exactly coinciding with the fundamental and harmonics of the large-signal stimulus. The on-frequency technique requires more than a single measurement because, with one measurement, the part of the output wave resulting from a_{gh} is indistinguishable from the part of the output resulting from a_{gh}^* . Two orthogonal input perturbations can be used to distinguish this, since the components in the outputs can then be mathematically decomposed into terms resulting from the individual exponential component inputs. In addition, a useful technique to reduce noise in the measurement is to “overdetermine” the result by measuring the output due to cosines with several phases and then use a least-squares fit to determine the exact solution [9]. Both the on-frequency and off-frequency measurement techniques are used in different instrumentation solutions.

To summarize, the process for measuring X-parameters is as follows based on the formulation of the defining equation (4):

- 1) Terminate all ports and harmonics in Z_0 loads and apply a large-signal input to port 1 and harmonic 1 (A_{11}). Measure the output signals (magnitude and phase) at all harmonics and all ports. Correct the phase terms appropriately for harmonic differences. This gives the $X_{ef}^{(F)}$ matrix. Each parameter in this matrix is a complex parameter, so magnitude and phase measurements of the output harmonics are necessary.
- 2) For each combination of input port and harmonic and output port and harmonic, perform the following steps: With all ports terminated in Z_0 and A_{11} still applied to the input, apply a perturbation signal consisting of terms a_{gh} and a_{gh}^* synchronized in phase with A_{11} to each port g and harmonic h ; this input should have a frequency slightly but distinguishably above harmonic h . For this input, measure the output magnitude (and phase if possible) of the output terms above and below each port e and harmonic f . The voltage traveling wave is measured at the frequency slightly above the harmonic, divided by a_{gh} (the phasor of the input cosine), and corrected for phase (as given by the equation), gives $X_{ef,gh}^{(S)}$. The voltage traveling wave measured at the frequency slightly below the harmonic, divided by a_{gh}^* and corrected for phase (as given by the equation), gives $X_{ef,gh}^{(T)}$.

For the simple case of two ports and three harmonics, the matrix equation appears as shown at the top of the following page. In many cases, five harmonics are used for the measurement. This requires finding an $X^{(F)}$ vector of 10 elements and $X^{(S)}$ and $X^{(T)}$ vectors of size 10×10 (100 elements each). This means that the total number of X-parameters that must be found in a two-port, five-harmonic system is 210.

$$\begin{bmatrix} B_{11} \\ B_{12} \\ B_{13} \\ B_{21} \\ B_{22} \\ B_{23} \end{bmatrix} = \begin{bmatrix} X_{11}^{(f)} P \\ X_{12}^{(f)} P^2 \\ X_{13}^{(f)} P^3 \\ X_{21}^{(f)} P \\ X_{22}^{(f)} P^2 \\ X_{23}^{(f)} P^3 \end{bmatrix} + \begin{bmatrix} X_{11}^{(s)} & X_{11,12}^{(s)} P^{-1} & X_{11,13}^{(s)} P^{-2} & X_{11,21}^{(s)} & X_{11,22}^{(s)} P^{-1} & X_{11,23}^{(s)} P^{-2} \\ X_{12,11}^{(s)} P & X_{12,12}^{(s)} & X_{12,13}^{(s)} P^{-1} & X_{12,21}^{(s)} & X_{12,22}^{(s)} & X_{12,23}^{(s)} P^{-1} \\ X_{13,11}^{(s)} P^2 & X_{13,12}^{(s)} P & X_{13,13}^{(s)} & X_{13,21}^{(s)} P^2 & X_{13,22}^{(s)} P^1 & X_{13,23}^{(s)} \\ X_{21,11}^{(s)} & X_{21,12}^{(s)} P^{-1} & X_{21,13}^{(s)} P^{-2} & X_{21,21}^{(s)} & X_{21,22}^{(s)} P^{-1} & X_{21,23}^{(s)} P^{-2} \\ X_{22,11}^{(s)} P & X_{22,12}^{(s)} & X_{22,13}^{(s)} P^{-1} & X_{22,21}^{(s)} P & X_{22,22}^{(s)} & X_{22,23}^{(s)} P^{-1} \\ X_{23,11}^{(s)} P^2 & X_{23,12}^{(s)} P & X_{23,13}^{(s)} & X_{23,21}^{(s)} P^2 & X_{23,22}^{(s)} P & X_{23,23}^{(s)} \end{bmatrix} \begin{bmatrix} a_{11} \\ a_{12} \\ a_{13} \\ a_{21} \\ a_{22} \\ a_{23} \end{bmatrix} \\
+ \begin{bmatrix} X_{11,11}^{(t)} P^2 & X_{11,12}^{(t)} P^3 & X_{11,13}^{(t)} P^4 & X_{11,21}^{(t)} P^2 & X_{11,22}^{(t)} P^3 & X_{11,23}^{(t)} P^4 \\ X_{12,11}^{(t)} P^3 & X_{12,12}^{(t)} P^4 & X_{12,13}^{(t)} P^5 & X_{12,21}^{(t)} P^3 & X_{12,22}^{(t)} P^4 & X_{12,23}^{(t)} P^5 \\ X_{13,11}^{(t)} P^4 & X_{13,12}^{(t)} P^5 & X_{13,13}^{(t)} P^6 & X_{13,21}^{(t)} P^4 & X_{13,22}^{(t)} P^5 & X_{13,23}^{(t)} P^6 \\ X_{21,11}^{(t)} P^2 & X_{21,12}^{(t)} P^3 & X_{21,13}^{(t)} P^4 & X_{21,21}^{(t)} P^2 & X_{21,22}^{(t)} P^3 & X_{21,23}^{(t)} P^4 \\ X_{22,11}^{(t)} P^3 & X_{22,12}^{(t)} P^4 & X_{22,13}^{(t)} P^5 & X_{22,21}^{(t)} P^3 & X_{22,22}^{(t)} P^4 & X_{22,23}^{(t)} P^5 \\ X_{23,11}^{(t)} P^4 & X_{23,12}^{(t)} P^5 & X_{23,13}^{(t)} P^6 & X_{23,21}^{(t)} P^4 & X_{23,22}^{(t)} P^5 & X_{23,23}^{(t)} P^6 \end{bmatrix} \begin{bmatrix} a_{11}^* \\ a_{12}^* \\ a_{13}^* \\ a_{21}^* \\ a_{22}^* \\ a_{23}^* \end{bmatrix}$$

Applications and Practical Limitations of Nonlinear Network Parameters

The goal of the nonlinear parameters is to facilitate the design of nonlinear circuits (i.e., amplifiers and systems) with simulation techniques and without the use of a circuit-element-based compact model. The parameters are directly extracted by measurements and are used to form a measurement-based model [14]. Nonlinear parameters extend the paradigm for S-parameters using small-signal design to the large-signal regime, and may reduce the dependence on complicated nonlinear modeling of systems in many cases.

With this in mind, Agilent Technologies [15] and Applied Wave Research (AWR) [16] have both provided for simulation of nonlinear devices using their X-parameter files. AWR also includes the capability to read in S-function data and results from waveform engineering measurements. The nonlinear parameter files can be entered into the Advanced Design System (ADS) or AWR Microwave Office software and simulated within a circuit environment. Much work using X-parameters to this point has been performed on system components (i.e., packaged amplifiers), and a feature of the X-parameter approach is that X-parameters of subsystems can be cascaded in the simulator to allow simulation of entire receiver or transmitter designs.

Applications

For small-signal amplifier operation, amplifier gain characteristics, such as the operating power gain, G_p , can be described completely in terms of the S-parameters and the load and source reflection coefficients

$$G_p = \frac{1}{1 - \Gamma_{IN}} |S_{21}|^2 \frac{1 - |\Gamma_L|^2}{|1 - S_{22}\Gamma_L|^2}, \quad (7)$$

where

$$\Gamma_{Ms} = \frac{B_1 \pm \sqrt{B_1^2 - 4|C_1|^2}}{2C_1}$$

and

$$\Gamma_{ML} = \frac{B_2 \pm \sqrt{B_2^2 - 4|C_2|^2}}{2C_2},$$

and B_1 , B_2 , C_1 , and C_2 are also functions of the S-parameters [7]. It seems that a natural extension of describing the nonlinear behavior of the device through a set of parameters would be to describe the gain in terms of these parameters. It is likely that other desired nonlinear performance criteria, such as stability, third-order intercept (TOI), and adjacent-channel power ratio (ACPR) may also be able to be described in terms of nonlinear parameters.

The ability to simulate contours easily for different nonlinear gain criteria will move nonlinear design from predominantly empirical techniques to an approach that is more heavily analytical. The tradeoff between linearity and efficiency in power amplifiers is presently a critical issue in both communication and radar systems. Device nonlinearities in transmitter power amplifiers lead to unwanted spectral spreading. This can cause the transmitter to violate spectral mask requirements set by regulatory agencies such as the U.S. Federal Communications Commission (FCC) or the U.S. Radar Spectrum Evaluation Criteria (RSEC) [19], [20]. However, amplifiers must be designed with high efficiency to minimize wasting supply power and causing it to be dissipated as heat, causing thermal issues in base station transmitters. If designers have the ability to simulate efficiency contours and ACPR contours (describing linearity), linearity-efficiency trade-off considerations in design will be made easier. Efficiency can be maximized while ensuring that the design meets spectral mask requirements through a visual trade-off process made evident on the Smith chart.

Limitations

The X-parameters in (4) form a basic nonlinear platform for nonlinear device characterization. However, real

nonlinear radio frequency (RF) devices do not exhibit time-invariant behavior. Because of slow thermal and trapping effects in the device itself, the device characteristics, and hence its X-parameters, are dependent on the slow process states of the device. These effects are known within the power amplifier design community as “memory effects.” The X-parameters have been modified by Verspecht et al. [17] to account for the possibility of the memory-effect time variance. Memory-effect modifications suggested in this approach are valid if the rate of change of the effect is significantly less than the modulation speed. A recent paper by Verspecht [18] also extends the X-parameter framework to be able to describe wideband modulated signals, or signals with an envelope that varies significantly longer than the time associated with slow memory effects (i.e., thermal, trapping, or bias modulation effects). Based on these developments, the memory effect issue no longer presents a theoretical imitation to the use of X-parameters. However, the memory-effect model has not yet been implemented in some software and nonlinear VNA solutions.

Another issue in the use of the X-parameters for strongly nonlinear applications is that a limited number of harmonics are usually measured. When only four or five harmonics of the system are measured, designers must keep in mind that extreme nonlinearities should be treated with caution. In addition, it should be noted by designers that the use of 50- Ω X-parameter data to predict behavior around the entire Smith Chart is limited. The ability to use load-pull in conjunction with X-parameters, however, is helpful in predicting the load-impedance variation of the nonlinear device characteristics. A recent paper by Simpson [21] illustrates how load-pull, that is, variation of the load impedance, can be used in conjunction with X-parameter measurements to allow the behavior of the device to be accurately characterized for high reflection coefficients.

Conclusions

The advent of the nonlinear network parameters provides a platform that promises new innovations for the nonlinear circuit design cycle. These parameters characterize a device, circuit, or system according to a black box approach, using the measured port characteristics to generate a simulation model for the device. The use of the nonlinear network parameters is expected to significantly shorten the design process and, in turn, provide savings of money and time for companies. While useful, the potential and limitations of these approaches must be realistically understood so that these techniques can be properly applied.

Acknowledgments

The authors are grateful to Loren Betts of Agilent Technologies and to the editors and reviewers of *IEEE*

Microwave Magazine for their insightful comments and assistance related to this article.

References

- [1] D. Root. (2009, April). A new paradigm for measurement, modeling, and simulation of nonlinear microwave and RF components. presented at Berkeley Wireless Research Center Seminar. [Online]. Available: <http://bwrc.eecs.berkeley.edu/php/pubs/pubs.php/1130.html>
- [2] G. Pailloncy, F. Verbeyst, and M. Vanden Bossche, “Nonlinear extensions for VNAs: Quid pro quo?” *Microwave J.*, vol. 52, no. 9, pp. 118–128, Sept. 2009.
- [3] M. Myslinski, F. Verbeyst, M. Vanden Bossche, and D. Schreurs, “S-functions extracted from narrow-band modulated large-signal network analyzer measurements,” in *74th Automatic RF Techniques Group Conf. Dig.*, Dec. 2009, pp.1–8.
- [4] F. Verbeyst and M. Vanden Bossche, “VIOMAP: The S-parameter equivalent for weakly nonlinear RF and microwave devices,” *IEEE Trans. Microwave Theory Tech.*, vol. 42, no. 12, pp. 2531–2535, Dec. 1994.
- [5] P. Tasker, “Practical waveform engineering,” *IEEE Microwave Mag.*, vol. 10, no. 7, pp. 65–76, Dec. 2009.
- [6] D. Root, J. Horn, L. Betts, C. Gillease, and J. Verspecht, “X-parameters: The new paradigm for measurement, modeling, and design of nonlinear RF and microwave components,” *Microwave Eng. Eur.*, vol. 51, no. 12, pp.16–21, Dec. 2008.
- [7] G. Gonzalez, *Microwave Transistor Amplifiers: Analysis and Design*, 2nd ed. Englewood Cliffs, NJ: Prentice-Hall, 1997.
- [8] D. Vye, “Fundamentally changing nonlinear microwave design,” *Microwave J.*, vol. 53, no. 3, pp. 22–44, Mar. 2010.
- [9] J. Verspecht, D. J. Williams, D. Schreurs, K.A. Remley, and M. McKinley, “Linearization of large-signal scattering functions,” *IEEE Trans. Microwave Theory Tech.*, vol. 53, no. 4, Apr. 2005, pp. 1369–1376.
- [10] J. Verspecht and D. Root, “Polyharmonic distortion modeling,” *IEEE Microwave Mag.*, vol. 7, no. 3, pp. 44–57, June 2006.
- [11] E. Chu, “Index mapping and mixed-radix FFTs,” in *Discrete and Continuous Fourier Transforms: Analysis, Applications and Fast Algorithms*. Boca Raton, Florida: Chapman and Hall/CRC, 2008, pp. 314–320.
- [12] E. Saff and A. Snider, *Fundamentals of Complex Analysis with Applications to Engineering and Science*, 3rd ed. Upper Saddle River, New Jersey: Pearson Education Inc., 2003.
- [13] R. J. Marks II, *Handbook of Fourier Analysis and Its Applications*. London, U.K.: Oxford Univ. Press, 2009.
- [14] D. Schreurs, J. Verspecht, B. Nauwelaers, A. Van de Capelle, and M. Van Rossum, “Direct extraction of the non-linear model for two-port devices from vectorial non-linear network analyzer measurements,” in *27th European Microwave Conf. Dig.*, Sept. 1997, pp. 921–926.
- [15] Agilent Technologies, Santa Rosa, CA. Available: <http://www.agilent.com>
- [16] Applied Wave Research, El Segundo, CA. Available: <http://web.awrcorp.com>
- [17] J. Verspecht, J. Horn, L. Betts, D. Gunyan, R. Pollard, C. Gillease, and D. Root, “Extension of X-parameters to include long-term dynamic memory effects,” in *IEEE MTT-S Int. Microwave Symp. Dig.*, Boston, MA, June 2009, pp. 741–744.
- [18] J. Verspecht, J. Horn, and D. Root, “A simplified extension of X-parameters to describe memory effects for wideband modulated signals,” in *Automatic RF Techniques Group (ARFTG) Conf. Dig.*, Anaheim, CA, May 2010, pp. 1–6.
- [19] J. de Graaf, H. Faust, J. Alatishe, and S. Talapatra, “Generation of spectrally confined transmitted radar waveforms,” in *Proc. IEEE Radar Conf.*, Apr. 24–27, 2006, pp. 76–83.
- [20] C. Baylis, L. Wang, M. Moldovan, J. Martin, H. Miller, L. Cohen, and J. de Graaf, “Designing for spectral conformity: Issues in power amplifier design,” in *Proc. IEEE Waveform Diversity Conf.*, Niagara Falls, Ontario, Canada, Aug. 2010, pp. 220–223.
- [21] G. Simpson, “High power load pull with X-parameters – A new paradigm for modeling and design,” in *Proc. IEEE Wireless and Microwave Technology Conf.*, Melbourne, FL, Apr. 2010, pp. 1–4. 